IEEE Access
Multidisciplinary | Rapid Review | Open Access Journal

Received October 12, 2020, accepted October 16, 2020, date of publication October 23, 2020, date of current version April 20, 2021.

Digital Object Identifier 10.1109/ACCESS.2020.3033319

Power Flow Calculation and Conductor Temperature Change Process Analysis of Single-Line Direct Supply Traction Network

LIJUN SUN[1,2], RUOPENG ZHANG[2], MINGXING TIAN[2,3], HUIYING ZHANG[2], WENJUN TIAN[2], AND JINYANG XU[2]

[1]Key Laboratory of Opto-Technology and Intelligent Control, Ministry of Education, Lanzhou Jiaotong University, Lanzhou 730070, China
[2]School of Automation and Electrical Engineering, Lanzhou Jiaotong University, Lanzhou 730070, China
[3]Rail Transit Electrical Automation Engineering Laboratory of Gansu Province, Lanzhou Jiaotong University, Lanzhou 730070, China

Corresponding author: Mingxing Tian (tianmingxing@mail.lzjtu.cn)

This work was supported in part by the National Natural Science Foundation of China under Grant 51367010 and Grant 51867012, in part by the Science and Technology Program of Gansu Province, China, under Grant 17JR5RA083, and in part by the Program for Excellent Team of Scientific Research in Lanzhou Jiaotong University, China, under Grant 201701.

ABSTRACT The accuracy of the power flow calculation results of a traction network is closely related to the impedance parameters of the transmission wires of the network, and such parameters change dynamically under the influence of current and geographical and climatic conditions. To make the selection of transmission wires model and the calculation results of power flow highly accurate and congruent with the reality, the theory of electro-thermal coupling is introduced into the calculation of power flow in the traction network, and a power flow calculation method considering the influence of electro-thermal coupling is proposed in this paper. Firstly, the electro-thermal coupling principle of the traction network transmission line is analysed. Secondly, with a single-line direct power supply traction network as an example, the power flow calculation method and realisation process are introduced in detail in consideration of the influence of electro-thermal coupling. Thirdly, the universality of the power flow calculation method is investigated. Lastly, the degree of influence of current and geographical and climatic conditions on the resistance of transmission wires in the traction network and the results of power flow calculations are analysed in the form of examples. Results show that the resistance and maximum allowable continuous current carrying capacity of the traction network are greatly affected by geographical and climatic conditions. The change in transmission wire resistance should be considered in the process of power flow calculation of traction networks.

INDEX TERMS Electro-thermal coupling, Heat balance equation, Newton-Raphson method, Power flow calculation, Traction power supply.

NOMENCLATURE

A. PARAMETERS

m	Mass of the transmission wire per unit length [kg· m^{-1}].
C_p	Specific heat capacity of the transmission wire material [J.kg^{-1}· $^{\circ-1}$].
r_{ref}	Manufacturer-supplied reference values for the resistance [Ω· m^{-1}].
α_l	Temperature coefficient of conductor resistance [$^{\circ-1}$].
T_d	Manufacturer-supplied reference values for the temperature [°].
D_0	Outside diameter of the conductor [m].
K_{angle}	Wind direction factor [no unit].
ρ_f	Density of air [kg·m^{-3}].
V_w	Wind speed [m·s^{-1}].
μ_f	Absolute viscosity of air [kg·m^{-1}·s^{-1}].
k_f	Thermal conductivity of air [W·m^{-1}.$^{\circ-1}$].
T_a	Ambient temperature [°].
ε	Emissivity [no unit].
α	Solar absorptivity [no unit].
φ	Wind direction angle [deg].
Q_{se}	Solar radiation intensity [W·m^{-2}].

The associate editor coordinating the review of this manuscript and approving it for publication was Xiaodong Liang.

θ Effective incidence angle of the sun [deg].
A Projected area of the conductor [$m^2 \cdot m^{-1}$].
T_{max} Maximum allowable temperature [°].
ε_e Iterative accuracy of Newton Raphson method for power flow calculation.

B. VARIABLES

l_1, l_n Distance between the train and the traction substation [km].
$\dot{U}_k$ The k-th train terminal voltage, where k = 1,2. . .,n.
$\dot{U}_0$ Voltage vector at the low-voltage side of the traction transformer [kV].
Z_k The k-th equivalent impedances of the traction network, where k = 1,2. . .,n.
R_k The k-th equivalent resistance, where k = 1,2. . .,n.
X_k The k-th equivalent reactance of the traction network, where k = 1,2. . .,n.
Z_C Self-impedance of the contact wire per unit length [$\Omega \cdot km^{-1}$].
Z_T Self-impedance of the rail per unit length [$\Omega \cdot km^{-1}$].
Z_{CT} Mutual impedance between the contact wire and the rail per unit length [$\Omega \cdot km^{-1}$].
T Temperature of the transmission wire [°C].
P_g Active power of train g.
Q_g Reactive power of train g.
G_{gh} Real part of the node admittance matrix element Y_{gh} in Eq. (3).
B_{gh} Imaginary part of the node admittance matrix element Y_{gh} in Eq. (3).
e Real part of the train terminal voltage phasor.
f Imaginary part of the train terminal voltage phasor.
k Steps of iterations.
Δz_k Parameter correction for the k-th iteration.
$x_1 \sim x_n$ Distance between the train and the AT station [km].
D Distance between two adjacent AT stations [km].

C. FUNCTIONS

r_a Resistance value of the unit-length transmission wire [$\Omega \cdot m^{-1}$].
p_c Convection heat dissipation power per unit-length transmission line [$W \cdot m^{-1}$].
p_r Radiation heat dissipation power per unit-length transmission line [$W \cdot m^{-1}$].
p_s Absorption power per unit-length transmission line [$W \cdot m^{-1}$].
I_{max} Maximum allowable continuous carrying current of transmission wire [A].
ΔP_g Iterative deviations of the output active power of the node in the location of train g.
ΔQ_g Iterative deviations of the output reactive power of the node in the location of train g.
I_{gh} Current flowing through line gh [A].
I_g Current of section g traction network's transmission wire [A].

I. INTRODUCTION

The accuracy of power flow calculation results of traction networks is of great significance to the construction of traction networks, assessment of system reliability, and compilation of train diagrams. With the rapid development of high-speed railways in recent years, the construction of such railways under complex geographical and climatic conditions has become the focus of numerous scientific research. Take the Sichuan–Tibet Railway being constructed in China as an example. The geographical and climatic conditions of the Sichuan–Tibet railway are complicated, because of factors affecting altitude, tunnels, long ramps, temperature differences, and strong wind. In particular, the range of altitude rapidly changes from 500 to 5100 m, and the maximum wind speed can reach 35 meters per second. The temperature can reach 40 °C in summer and 20 °C below zero in winter, and the temperature difference between day and night can reach 35 °C. The temperature within the tunnel can reach 58 °C. Under such complicated geographical and climatic conditions, the accurate calculation of the traction network's power flow becomes extremely challenging.

In 2005, Canadian scholars Banakar H. and Alguacil N. proposed the concept and application framework of electro-thermal coupling in the operation of power systems. Their studies (Refs. [1], [2]). proved that wire current and meteorological conditions, such as ambient temperature, wind speed, and light intensity greatly influence conductor resistance. In the process of power flow calculation, the influence of the electro-thermal coupling on the transmission wire is taken into account and the resistance parameters of the transmission wire in the traction network are calculated in real-time, which can improve the accuracy of the power flow calculation results.

The influence of electro-thermal coupling on the resistance parameters of overhead transmission lines was analysed in Ref. [3], the results showed that the resistance and temperature of the transmission lines change together with the variations of the power load and environmental parameters of the wires. Refs. [4], [5] pointed out that electro-thermal coupling considerably affects the power flow calculation results of distribution networks, and the power flow calculation based on the constant resistance parameter will cause great error. The power flow calculation results of distribution networks were applied to the optimal dispatching of these networks in Refs. [6], [7], the results showed that the influence of electro-thermal coupling, when considered in the scheme, can dramatically affect the optimal dispatching of distribution networks. Refs. [8], [9] integrated the influence of electro-thermal coupling into the fields of wind power generation and photovoltaic power generation to improve wire capacity

utilization and power flow calculation accuracy. Apart from the results from the studies mentioned above, the application of electro-thermal coupling theory in the fields of dynamic thermal rating (Refs. [10]–[12]), stress analysis of conductors (Ref. [13]), and state assessments (Ref. [14]) has achieved certain levels of progress. Their corresponding results showed that the temperature and resistance of transmission wires vary with current, ambient temperature, light intensity, wind speed, and other conditions of the external environment. The resistance parameters should be corrected according to the wires' temperature in the power flow calculation process. Electro-thermal coupling theory has been applied to power systems. However, the resistance of transmission wires and the temperature of traction networks are also affected by environmental conditions and wire current. The application of electro-thermal coupling theory to the power flow calculation of traction networks is presently limited.

The power flow calculation of traction networks has been used as basis for the reliability analysis and system design of traction power supply systems. Scholars from around the world have conducted numerous studies in these areas and achieved good results (Refs [15]–[24]). In Refs. [16]–[19], the traction network in the power flow calculation process of a traction network was set equivalent to a previously reported lumped parameter model. In Ref. [20], the traction network was set as equivalent to the multi-conductor transmission line model. The chain equivalent circuit model was adopted in Refs. [21], [22], while the multiport equivalent circuit model was adopted in Refs. [23], [24]. The above studies have all focused on the traction network models, but they have not considered the influences of the current-carrying wires and environmental conditions of the traction network on the wires' impedance parameters. The impedance parameters of a traction network's transmission line vary with the load and environmental parameters of the wire. If the variations in the impedance parameters of the conductor is not considered in the power flow calculation process, then the error of the calculation results will be large.

Given the above mentioned background, this study introduces electro-thermal coupling theory into the power flow calculation of the traction network. On the basis of the traditional Newton–Raphson power flow calculation, the calculation link of the resistance parameters of the transmission lines is introduced to vary these parameters with the load and the surrounding environmental parameters of such transmission lines. In the process of power flow calculation, the change in the transmission wires' resistance is taken as the link, while the electric heating coupling equation and the power flow calculation are taken as the core. The relationships among power flow, environmental conditions, and temperature change are determined in real time to guarantee that the power flow calculation process for the traction network is aligned with the actual situation. The introduction of electro-thermal coupling theory into the power flow calculation of the traction network is a new exploration, and it can obtain much more accurate results during power flow calculation.

II. EQUIVALENT CIRCUIT MODEL OF A TRACTION NETWORK

The schematic diagram of the single-line direct power supply traction network is shown in Fig. 1. In sinusoidal steady state, $\dot{U}_0$ represents the voltage phasor at the low-voltage side of the traction transformer, such that $\dot{U}_0 = 27.5\angle 0°\text{kV}$.

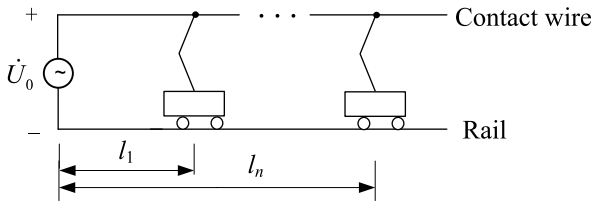

FIGURE 1. Schematic diagram of the single-line direct power supply traction network.

The train is the load of the traction network. The traction network can be regarded an active two-port network, that is, the traction network is equivalent to the series of voltage sources and impedances. If the terminal voltage of the former train is regarded the power supply voltage of the latter train, then the traction network between two trains can also be regarded equivalent to an impedance. Therefore, the traction network with a single-line direct power supply can be generally taken as equivalent to the circuit model, as shown in Fig. 2. Suppose the number of trains in a traction power supply arm is n, and the trains are regarded to have a constant power load, that is, the nodes where the trains take the current (nodes 1 to n in Fig. 2.) are PQ nodes; $\dot{U}_0$ is the voltage at the low-voltage side of the traction transformer, that is, node 0 is the balance node.

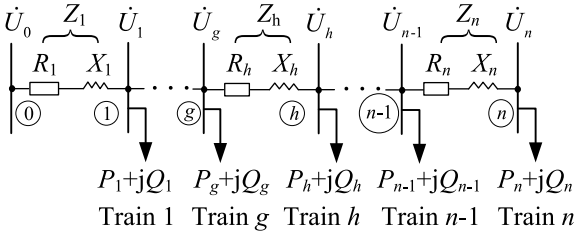

FIGURE 2. Equivalent circuit model of the traction network with a single-line direct power supply.

The equivalent impedance of the traction network is related to the parameters of wires per unit length of the traction network and the length from l_1 to l_n, as presented in Ref. [25]. The equivalent impedance of the unit-length traction network in the single-line direct power supply mode can be expressed as follows:

$$Z = z_C - \frac{z_{CT}^2}{z_T} \tag{1}$$

The equivalent impedance Z_g between any adjacent node g and h shown in Fig. 2 can be expressed as follows:

$$Z_g = (l_h - l_g)Z = (l_h - l_g)(z_C - \frac{z_{CT}^2}{z_T}) \tag{2}$$

where l_h and l_g are the distances from nodes h and g to the traction substation, respectively.

The node admittance matrix of the equivalent circuit model shown in Fig. 2 can be expressed as follows:

$$Y = \begin{bmatrix} Z_1^{-1} & -Z_1^{-1} & \cdots & 0 \\ -Z_1^{-1} & Z_1^{-1}+Z_2^{-1} & \cdots & 0 \\ 0 & \ddots & \ddots & 0 \\ 0 & \cdots & Z_{n-1}^{-1}+Z_n^{-1} & -Z_n^{-1} \\ 0 & \cdots & -Z_n^{-1} & Z_n^{-1} \end{bmatrix} \tag{3}$$

As the wire parameters of the traction network are a function of the wires' temperature, the equivalent impedance of the traction network is also a function of the wires' temperature. Similarly, the elements of the nodal admittance matrix are a function of the wires' temperature.

III. PRINCIPLE OF ELECTRO-THERMAL COUPLING OF THE TRANSMISSION WIRE OF THE TRACTION NETWORK

A. HEATING PROCESS OF THE TRACTION NETWORK's TRANSMISSION WIRE

This section is based on the thermal balance theory of transmission lines, as introduced in the IEEE-738 standard (Ref. [26]). The electro-thermal coupling block diagram of the transmission wire is shown in Fig. 3. Affected by the surrounding environment and the current, the temperature of the overhead transmission wire rises and causes a change in wire resistance. In turn, the current of the transmission wire is also affected. Thus, a coupling relationship exists between wire current and temperature.

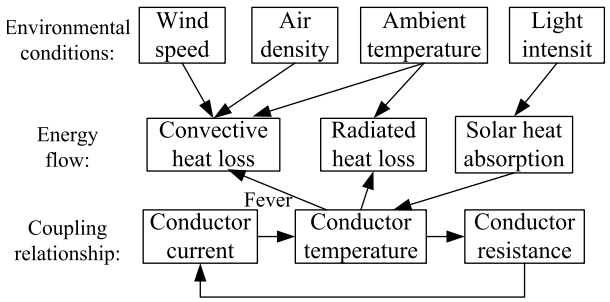

FIGURE 3. Electro-thermal coupling block diagram of the transmission wire.

When no current exists in the transmission wire of the traction network, the wire temperature is regarded equal to the ambient temperature of the wire. By contrast, when current exists, the current will cause the wire to heat up, causing the wire temperature to be higher than the ambient temperature. At the same time, the wire itself will dissipate heat into the surrounding environment and absorb solar radiation energy. The heat balance equation of the transmission wire in the traction network can be expressed as follows:

$$mC_p \frac{\mathrm{d}T}{\mathrm{d}t} = I^2 r_a + p_s - p_c - p_r \tag{4}$$

The relationship between wire resistance and wire temperature is as follows:

$$r_a = r_{\mathrm{ref}}[1 + \alpha_l (T - T_d)] \tag{5}$$

In Eq. (4), p_c, p_r, and p_s satisfy the following relationship:

$$\begin{cases} p_{c1} = K_{angle}[1.01 + 1.35(\frac{D_0 \rho_f V_w}{\mu_f})^{0.52}]k_f(T - T_a) \\ = A_{c1}(T - T_a) \\ p_{c2} = 0.754 K_{angle}(\frac{D_0 \rho_f V_w}{\mu_f})^{0.6} k_f (T - T_a) \\ = A_{c2}(T - T_a) \\ p_c = \max(p_{c1}, p_{c2}) = A_c(T - T_a) \end{cases} \tag{6}$$

$$p_r = 1.78 \cdot 10^{-9} D_0 \varepsilon [(T + 273)^4 - (T_a + 273)^4] \tag{7}$$

$$p_s = \alpha Q_{se} \sin(\theta) A \tag{8}$$

where, $K_{angle} = 1.194\text{-cos}\varphi + 0.194\cos 2\varphi + 0.368\sin 2\varphi$.

From Eqs. (4) ∼ (8), it can be seen that the wire resistance parameters are affected by wire temperature, while wire temperature is directly affected by the wire's current-carrying and the surrounding environmental parameters.

B. MAXIMUM ALLOWABLE CONTINUOUS CARRYING CURRENT OF THE TRANSMISSION WIRE

When the temperature of the transmission wire reaches the maximum allowable temperature (T_{max}) and is stabilized due to the influence of the current and the surrounding environment, the corresponding conductor current is regarded the maximum allowable continuous carrying current of this transmission wire (Ref. [27]). At this point, Eq. (4) can be expressed as follows:

$$I_{\max}^2 R_{\max} + p_s - p_c(T_{\max}) - p_r(T_{\max}) = 0 \tag{9}$$

According to Eq. (9), the maximum allowable continuous carrying current of transmission wire can be expressed as follows:

$$I_{\max} = \sqrt{\frac{p_c(T_{\max}) + p_r(T_{\max}) - p_s}{R_{\max}}} \tag{10}$$

Calculating for Eq. (10), combined with the maximum allowable temperature of the wire, indicates that the allowable continuous carrying capacity of this wire is mainly affected by its environmental parameters. Thus, the maximum allowable carrying capacity of the transmission wires should be determined comprehensively according to the environmental parameters of the wires across different seasons.

C. COUPLING RELATIONSHIP BETWEEN WIRES TEMPERATURE AND POWER FLOW IN THE TRACTION NETWORK

The terminal voltage of the train can be expressed as $\dot{U}_g = e_g + \mathrm{j}f_g$ (g$\in n$). The equation for the traditional power

flow calculation is given by:

$$\begin{cases} \Delta P_g = P_g - e_g \sum_{h=0}^{n} (G_{gh}e_h - B_{gh}f_h) \\ \quad -f_g \sum_{h=0}^{n} (G_{gh}f_h - B_{gh}e_h) = 0 \\ \Delta Q_g = Q_g - f_g \sum_{h=0}^{n} (G_{gh}e_h - B_{gh}f_h) \\ \quad +e_g \sum_{h=0}^{n} (G_{gh}f_h - B_{gh}e_h) = 0 \end{cases} \quad (\mathrm{g} = 1, 2, \ldots, n) \quad (11)$$

The unknown variables in Eq. (11) are the real part e and the imaginary part f of the train terminal voltage phasor. Eq. (11) can be abbreviated as follows:

$$m_g(e, f) = 0 (\mathrm{g} = 1, 2, \ldots, 2\mathrm{n}). \quad (12)$$

where e and f can be expressed as follows:

$$e = [e_1, e_2, \ldots, e_n], \quad (13)$$

$$f = [f_1, f_2, \ldots, f_n]. \quad (14)$$

In Fig. 2, the current flowing through line gh is expressed as follows:

$$I_{gh} = \sqrt{\frac{(e_g - e_h)^2 + (f_g - f_h)^2}{R_g^2 + X_g^2}}. \quad (15)$$

As depicted in Eq. (3), the elements of the nodal admittance matrix are affected by wire temperature; thus, the train's terminal voltage are also affected by the transmission wires' temperature. As shown in Eq. (15), the line's current is related to the train's terminal voltage and the wire's impedance, and all of them are affected by the wire's temperature. Thus, the line current changes together with the wire temperature. In turn, the wire current leads to a change in wire temperature. The above changes reflect the process of electrical and thermal coupling. When calculating the power flow of the traction network, the temperature change in the transmission wires of the traction network should be taken into account.

IV. POWER FLOW CALCULATION OF THE TRACTION NETWORK AND ANALYSIS OF THE TEMPERATURE CHANGE PROCESS OF THE TRANSMISSION WIRE

A. DYNAMIC POWER FLOW CALCULATION MODEL THAT CONSIDERS THE INFLUENCE OF ELECTRO-THERMAL COUPLING

When traction load and environmental conditions change, the coupling relationship between the current and the temperature of the transmission wire satisfies the dynamic differential equation given by Eq. (4). The differential equation can be solved using the difference method, and the differential equation can be discretized into an algebraic equation. Eq. (4) is discretized as follows:

$$mC_p(T_t - T_{t-\Delta t}) = \frac{\Delta t}{2}[I^2 r_a + p_s - p_c - p_r + I'^2 r'_a + p'_s - p'_c - p'_r]. \quad (16)$$

where T_t and $T_{t-\Delta t}$ represent the wire temperature at time t and time t-Δt, respectively; Δt is the difference time step; and p_s, p_c, and p_r are power at time t, while p'_s, p'_c, and p'_r are power at time t-Δt.

According to the analysis presented in Section C, the power flow of the traction network is related to wire temperature. Therefore, the equations for the temperature of the transmission wires can be introduced into the traditional power flow calculation. Eq. (16) can be written as the power flow calculation equation for the temperature of the transmission wire as follows:

$$\Delta E_h = T_{ht} - T_{h(t-\Delta t)} - \frac{\Delta t}{2mC_p}[I^2 r_{ah} + p_{hs} - p_{hc} - p_{hr} + I'^2 r'_{ah} + p'_{hs} - p'_{hc} - p'_{hr}] = 0 \quad (h = 1, 2, \ldots, n). \quad (17)$$

The current of the transmission line is related to the voltage of the train terminal. As such, Eq. (17) can be abbreviated as a function of the train's terminal voltage and wire temperature as follows:

$$n_h(e, f, T) = 0 \quad (\mathrm{h} = 1, 2, \ldots, n). \quad (18)$$

where $T = [T_1, T_2, \ldots, T_n]$ is a matrix corresponding to the temperature of the transmission wires.

The elements of the node admittance matrix are the functions of the temperature of the transmission wires. Thus, the traditional power flow calculation equation (Eq. (12)) can be regarded a function of the terminal voltage of the train and the temperature of the transmission wires. Eq. (12) can be written in the form of Eq. (19).

$$m_g(e, f, T) = 0 \quad (\mathrm{g} = 1, 2, \ldots, 2\mathrm{n}). \quad (19)$$

From Eqs. (18) and (19), the power flow calculation equation of the traction network that considers the effect of electro-thermal coupling can be uniformly expressed as follows:

$$S(z) = \begin{cases} \mathrm{M}(e, f, T) = \begin{cases} m_1(e, f, T) = 0 \\ m_2(e, f, T) = 0 \\ \vdots \\ m_{2n}(e, f, T) = 0 \end{cases} \\ N(e, f, T) = \begin{cases} n_1(e, f, T) = 0 \\ n_2(e, f, T) = 0 \\ \vdots \\ n_n(e, f, T) = 0 \end{cases} \end{cases} \quad (20)$$

where z is an unknown variable matrix, which can be expressed as $z = [efT]$.

The power flow calculation equation of the traction network by using the Newton–Raphson method can be written as follows:

$$S(z_k) = \frac{\partial S(z_k)}{\partial z_k} \Delta z_k = J \Delta z_k. \quad (21)$$

where J is the Jacobian matrix of function S(z) with respect to variable z,and it is a 3n-order matrix.

The Jacobian matrix element J_{ij} is defined as follows:

$$J_{ij} = \frac{\partial S_i}{\partial z_j} (\mathrm{i} \in 3\mathrm{n}, \mathrm{j} \in 3\mathrm{n}). \tag{22}$$

According to Eq. (21), the parameters correction (Δz_k) for the k-th iteration can be expressed as follows:

$$\Delta z_k = J_k^{-1} S(z_k). \tag{23}$$

The revised parameter after the k-th iteration can be written as follows:

$$z_{k+1} = z_k - \Delta z_k. \tag{24}$$

The iterative calculation is carried out repeatedly. The iteration ends when $|\Delta z_k| < \varepsilon_e$.

The Jacobian matrix J can be expressed as follows:

$$J = \begin{bmatrix} \frac{\partial \mathrm{M}}{\partial e} & \frac{\partial \mathrm{M}}{\partial f} & \frac{\partial \mathrm{M}}{\partial T} \\ \frac{\partial \mathrm{N}}{\partial e} & \frac{\partial \mathrm{N}}{\partial f} & \frac{\partial \mathrm{N}}{\partial T} \end{bmatrix} = \begin{bmatrix} J_k & \frac{\partial \mathrm{M}}{\partial T} \\ \frac{\partial \mathrm{N}}{\partial e} \quad \frac{\partial \mathrm{N}}{\partial f} & \frac{\partial \mathrm{N}}{\partial T} \end{bmatrix}. \tag{25}$$

where J_k is a traditional Jacobian matrix, and $\frac{\partial \mathrm{M}}{\partial T}$ is the partial derivative matrix of the traditional power flow equation with respect to the wire temperature T, which can be expressed as follows:

$$\frac{\partial \mathrm{M}}{\partial \mathrm{T}} = \begin{bmatrix} \frac{\partial \mathrm{m}_1}{\partial T_1} & \frac{\partial \mathrm{m}_1}{\partial T_2} & \cdots & \frac{\partial \mathrm{m}_1}{\partial T_n} \\ \frac{\partial \mathrm{m}_2}{\partial T_1} & \frac{\partial \mathrm{m}_2}{\partial T_2} & \cdots & \frac{\partial \mathrm{m}_2}{\partial T_1} \\ \vdots & \vdots & \ddots & \vdots \\ \frac{\partial \mathrm{m}_{2n}}{\partial T_1} & \frac{\partial \mathrm{m}_{2n}}{\partial T_2} & \cdots & \frac{\partial \mathrm{m}_{2n}}{\partial T_n} \end{bmatrix}. \tag{26}$$

As Eq. (19) is an abbreviated form of Eq. (11), the matrix elements in Eq. (26) can be expressed as $\frac{\partial \Delta P_g}{\partial T_k}$ and $\frac{\partial \Delta Q_g}{\partial T_k}$, Where g=1,2…$n$; k =1,2…n. As shown in Fig. 2, when the transmission wire k and node g meet the requirements of $k = g$ or $k = g+1$, wire k is associated with node g. In this case, the matrix elements in Eq. (26) can be expressed as follows:

$$\begin{cases} \frac{\partial \Delta P_g}{\partial T_k} = -e_g(\frac{\partial G_{gh}}{\partial T_k} e_h - \frac{\partial B_{gh}}{\partial T_k} f_h) - f_g(\frac{\partial G_{gh}}{\partial T_k} f_h \\ -\frac{\partial B_{gh}}{\partial T_k} e_h) - (e_g^2 + f_g^2)\frac{\partial G_{gg}}{\partial T_k} + 2e_g f_g \frac{B_{gg}}{\partial T_k} \\ \frac{\partial \Delta Q_g}{\partial T_k} = -f_g(\frac{\partial G_{gh}}{\partial T_k} e_h - \frac{\partial B_{gh}}{\partial T_k} f_h) + e_g(\frac{\partial G_{gh}}{\partial T_k} f_h \\ -\frac{\partial B_{gh}}{\partial T_k} e_h) + (f_g^2 - e_g^2)\frac{\partial B_{gg}}{\partial T_k}. \end{cases} \tag{27}$$

where $g = 1, 2 \ldots n$; $k = g$ or $k = g+1$. If $k = g$ then $h = g-1$, and if $k = g+1$, then $h = g+1$. G_{gh}, B_{gh}, G_{gg}, and B_{gg} represent mutual conductance, mutual susceptance, self-conductance, and self-susceptance, respectively. These four variables are functons of wire temperature T_k.

When transmission wire k is not associated with node g, both $\frac{\partial \Delta P_g}{\partial T_k}$ and $\frac{\partial \Delta Q_g}{\partial T_k}$ are equal to 0.

The Jacobian matrix elements $\frac{\partial \mathrm{N}}{\partial e}$ and $\frac{\partial \mathrm{N}}{\partial f}$ in Eq. (25) represent the deflection matrix of the conductor temperature equation (Eq. (18)) to the real part e and virtual part f of the train's terminal voltage phasor. These elements are specifically expressed as follows:

$$\frac{\partial \mathrm{N}}{\partial e} = \begin{bmatrix} \frac{\partial \mathrm{n}_1}{\partial e_1} & \frac{\partial \mathrm{n}_1}{\partial e_2} & \cdots & \frac{\partial \mathrm{n}_1}{\partial e_n} \\ \frac{\partial \mathrm{n}_2}{\partial e_1} & \frac{\partial \mathrm{n}_2}{\partial e_2} & \cdots & \frac{\partial \mathrm{n}_2}{\partial e_1} \\ \vdots & \vdots & \ddots & \vdots \\ \frac{\partial \mathrm{n}_n}{\partial e_1} & \frac{\partial \mathrm{n}_n}{\partial e_2} & \cdots & \frac{\partial \mathrm{n}_n}{\partial e_n} \end{bmatrix}, \tag{28}$$

$$\frac{\partial \mathrm{N}}{\partial f} = \begin{bmatrix} \frac{\partial \mathrm{n}_1}{\partial f_1} & \frac{\partial \mathrm{n}_1}{\partial f_2} & \cdots & \frac{\partial \mathrm{n}_1}{\partial f_n} \\ \frac{\partial \mathrm{n}_2}{\partial f_1} & \frac{\partial \mathrm{n}_2}{\partial f_2} & \cdots & \frac{\partial \mathrm{n}_2}{\partial f_1} \\ \vdots & \vdots & \ddots & \vdots \\ \frac{\partial \mathrm{n}_n}{\partial f_1} & \frac{\partial \mathrm{n}_n}{\partial f_2} & \cdots & \frac{\partial \mathrm{n}_n}{\partial f_n} \end{bmatrix}. \tag{29}$$

The matrix elements in Eqs. (28) and (29) have the following relationship:

$$\begin{cases} \frac{\partial \mathrm{n}_g}{\partial e_k} = -\frac{\Delta t}{2mC_p} \frac{\partial I_g^2}{\partial e_k} r_{ag} \\ \frac{\partial \mathrm{n}_g}{\partial f_k} = -\frac{\Delta t}{2mC_p} \frac{\partial I_g^2}{\partial f_k} r_{ag} \end{cases} (\mathrm{g}, \mathrm{k} = 1, 2, \ldots, \mathrm{n}). \tag{30}$$

When the transmission wire g is associated with node k, Eq. (30) equals 0.

In Eq. (30), the current I_g of section g traction network's transmission wire meets the following relationship:

$$I_g^2 = \frac{(e_g - e_{g-1})^2 + (f_g - f_{g-1})^2}{R_g^2 + X_g^2}. \tag{31}$$

$\frac{\partial \mathrm{n}_g}{\partial e_k}$ and $\frac{\partial \mathrm{n}_g}{\partial f_k}$ can be solved by bringing the formula (31) into the formula (30).

The matrix element $\frac{\partial \mathrm{N}}{\partial T}$ in Eq. (25) is the partial derivative matrix of the power flow calculation equation for temperature (Eq. (18)) with respect to temperature T. This element is a diagonal matrix, which can be expressed as follows:

$$\frac{\partial \mathrm{N}}{\partial T} = diag(\frac{\partial \mathrm{n}_1}{\partial T_1}, \frac{\partial \mathrm{n}_2}{\partial T_2}, \cdots, \frac{\partial \mathrm{n}_n}{\partial T_n}) \tag{32}$$

where the diagonal matrix element $\frac{\partial \mathrm{n}_g}{\partial T_g}$ is given by:

$$\frac{\partial \mathrm{n}_g}{\partial T_g} = 1 - \frac{\Delta t}{2mC_p}[\frac{\partial I_g^2}{\partial T_g} r_{ag} + \frac{\partial r_{ag}}{\partial T_g} I_g^2] - \frac{\partial p_{cg}}{\partial T_g} - \frac{\partial p_{rg}}{\partial T_g} \quad (\mathrm{g} = 1, 2, \ldots, \mathrm{n}). \tag{33}$$

B. IMPLEMENTATION OF THE ALGORITHM

The calculation process of traction network's power flow that considers the influence of electro-thermal coupling is shown in Fig. 4. The process of the power flow calculation includes three modules: system initialization, power flow calculation,

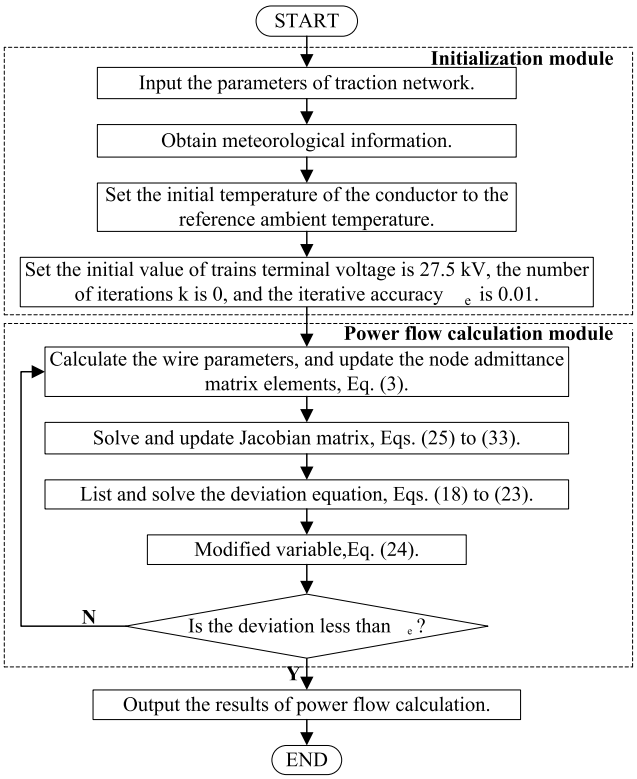

FIGURE 4. Flowchart of the traction network's power flow calculation that considers the influence of electro-thermal coupling.

and result output. In the process of power flow calculation, the meteorological parameters along the traction network need to be updated regularly. The National Meteorological Department can provide minute-level meteorological information to meet the algorithmic requirements.

1) INITIALIZATION MODULE

In the initialization module, it is necessary to input the relative position and parameter information of traction network transmission line, weather forecast information (ambient temperature, wind speed, wind direction, etc.) and set the initial value of conductor temperature and terminal voltage of train, as well as iterative accuracy.

2) POWER FLOW CALCULATION CONSIDERING THE ELECTRO-THERMAL COUPLING PRINCIPLE MODULE

The module is solved by Newton Raphson method. In the process of each iteration, firstly, the elements in the nodal admittance matrix are modified by Eqs. (1)-(3) and (5); secondly, the Jacobian matrix element is solved and updated by Eqs. (25)-(33); thirdly, the iteration deviation is calculated from Eqs. (18)-(23); finally, the variable is modified by Eq. (24).

3) RESULT OUTPUT MODULE

The train voltage and temperature of transmission wire are corrected repeatedly until the deviation are less than the iteration accuracy ε_e. after the iteration, the power flow calculation results of traction network are output.

V. GENERALITY OF THE ALGORITHM

In addition to the single-line direct power supply mode, the single-line AT (Auto Transformer) power supply mode and the AT power supply mode for the terminal's parallel double-tracks are also commonly used in traction networks. The single-line AT power supply mode is shown in Figure 5. As the ends of the uplink and the downlink traction network are parallel connection, the AT power supply mode for the terminal's parallel double-tracks can be simplified to the structure shown in Figure 6. Regardless of the power supply mode adopted, the train is regarded the load of the traction network, and the traction network can be regarded an active two-terminal network, so it can be equivalent to the equivalent circuit model shown in Figure 2. The impedance parameters in the equivalent circuit model under various power supply modes of the traction network can be calculated according to the relationship between the voltage drop and the current.

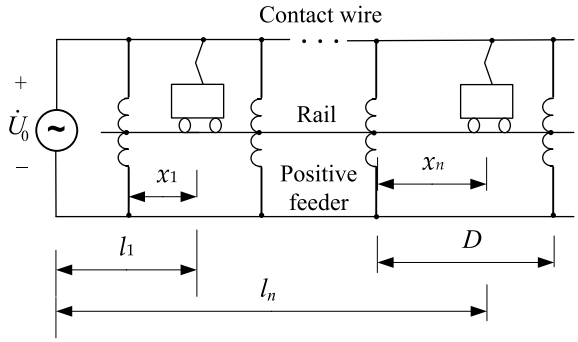

FIGURE 5. Schematic diagram of the single-line AT power supply traction network.

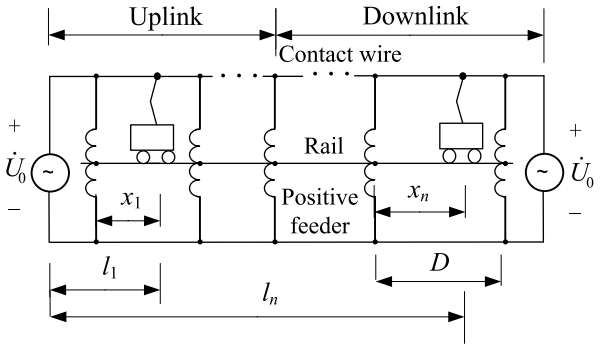

FIGURE 6. Schematic diagram in the AT power supply mode for the terminal parallel double-tracks.

As the traction network can be set equivalent to the circuit form shown in Fig. 2 in different power supply modes (Figs. 5 and 6), the power flow calculation method proposed in this study that considers the influence of electric heating coupling is also suitable.

VI. IDENTIFICATION OF METEOROLOGICAL PARAMETERS

The meteorological parameters selected in this study refer to the meteorological information products provided by the National Meteorological Information Center of China.

TABLE 1. Main Climatic Parameters in Lhasa.

Parameters	Spring		Summer		Autumn		Winter	
	Fixed value	Range	Fixed value	Range	Fixed value	Range	Fixed value	Range
V_w (m·s^{-1})	5.0	0 ~18	1.8	0 ~15	3.0	0 ~15	4.0	0 ~16
φ (deg)	45	0 ~90	45	0 ~90	45	0 ~90	45	0 ~90
T_a (°C^{-1})	15	5 ~29	33	20 ~40	10	2 ~20	-15	-25 ~-5
ρ_f(kg·m^{-3})	1.20	1.14 ~1.25	1.17	1.16~1.18	1.22	1.16~1.27	1.30	1.25~1.35

TABLE 2. Main Climatic Parameters in Nanjing.

Parameters	Spring		Summer		Autumn		Winter	
	Fixed value	Range	Fixed value	Range	Fixed value	Range	Fixed value	Range
V_w (m·s^{-1})	2.5	0 ~ 10	0.5	0 ~ 10	2.0	0 ~10	3.0	0 ~ 10
φ (deg)	45	0 ~90	45	0 ~90	45	0 ~90	45	0 ~90
T_a (°C^{-1})	25	15 ~ 32	36	20~ 40	27	15 ~ 32	8	-4 ~ 15
ρ_f(kg·m^{-3})	1.14	1.16 ~ 1.23	1.14	1.13 ~ 1.20	1.26	1.16 ~1.23	1.26	1.23 ~1.31

In recent years, the National Meteorological Department has developed various meteorological information products for relevant scientific research purposes and for other departments with practical needs. China has a large geographical span, and huge climatic differences exist between the south and north parts. In this study, the key climatic parameters of Lhasa and Nanjing are selected for analysis. The geographical coordinates of Lhasa are 91.06° E longitude and 29.36° N latitude at 3650 meters above sea level, belonging to the plateau-temperate semi-arid monsoon climate. Meanwhile, the geographical coordinates of Najing are 118.78° E longitude and 32.07° N latitude at 15 meters above sea level, and belonging to the subtropical monsoon climate. The climate difference between Lhasa and Nanjing is obvious. On the basis of the identified climatic parameters of the two places, this study compares and analyzes the current carrying, heating, and current distribution of the traction network transmission line given the geographical and climatic conditions of the two places.

As shown in Eqs. (6) to (8), the environmental parameters related to electro-thermal coupling are wind speed, wind direction angle, density of air, absolute viscosity of air, thermal conductivity of air, temperature of ambient air, and emissivity. The values of thermal conductivity of air and absolute viscosity of air are comparatively small. Emissivity is only related to the surface property of the wire. Therefore, these parameters have minimal effects on electro-thermal coupling. In this study, these parameters are constant in concordance with Ref. [26] with the following values:

Thermal conductivity of air, k_f: 0.025 (W·m^{-1}·°C^{-1}).

Absolute viscosity of air, μ_f: 2.043 × 10−5 (kg·m^{-1}·s).

Emissivity, ε: 0.5 (no unit).

As shown in Eq. (8), the solar radiation heat absorption power (p_s) is related to solar radiation intensity and effective incident angle. In Refs. [2∼8], the solar radiation heat absorption power is constant. In this study, the value of p_s is 22.44 (W ·m^{-1}).

The main environmental parameters that greatly influence electro-thermal coupling are wind speed, V_w; wind direction angle, φ; ambient temperature, T_a; and air density, ρ_f. The results of the historical climate data provided by the National Meteorological Information Center are statistically analyzed, and the fixed value in this study and the variation range of the environmental parameters in Lhasa and Nanjing are obtained. The results are shown in Tables 1 and 2. The ''fixed value'' in the tables represent environmental parametric values with high frequencies.

VII. CASE STUDIES

A. EXAMPLES WITH KNOWN CONDITIONS

A single-line, direct-power-supply traction system is considered. The voltage at the exit of the traction substation is 27.5kV, and the length of the single-side power supply arm is 20km. The type of contact wire is CTA. The diameter of the contact wire is 25.8mm, the temperature coefficient of conductor resistance (α_l) is 0.0039, the specific heat capacity of the transmission wire material(C_p) is 849 (J·kg^{-1}·°C^{-1}), and the maximum allowable working temperature of the contact wire is 150°C. The reference environmental parameters are as follows: the ambient temperature is 20°C, usage of standard atmospheric pressure, and no wind. Under the reference environmental parameters, the self-impedance of the contact wire per unit length is $z_C = 0.234 + \mathrm{j}0.53$ (Ω·km^{-1}), and the self-impedance of the rail per unit length is $z_T = 0.198 + \mathrm{j}0.56$ (Ω·km^{-1}). The mutual impedance between the contact wire and rail per unit length is $z_{CT} = 0.05 + \mathrm{j}0.319$ (Ω·km^{-1}). The parameters identified in Section 5 are adopted as the environmental parameters.

B. STATIC ANALYSIS

Case 1: The environmental parameters under the assumption that the OCS is located in Lhasa are shown in Table 1. The contact wire has a constant current of 500A, and the influence

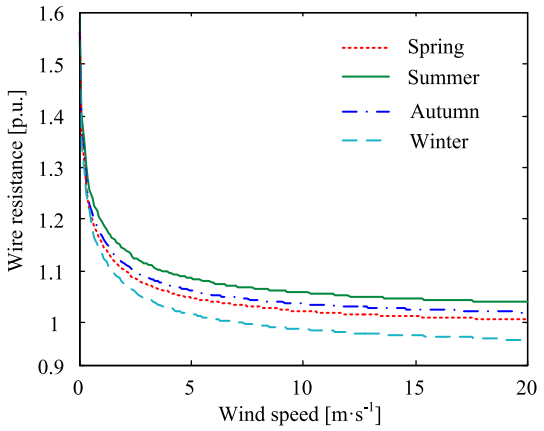

(a) Wind speed change

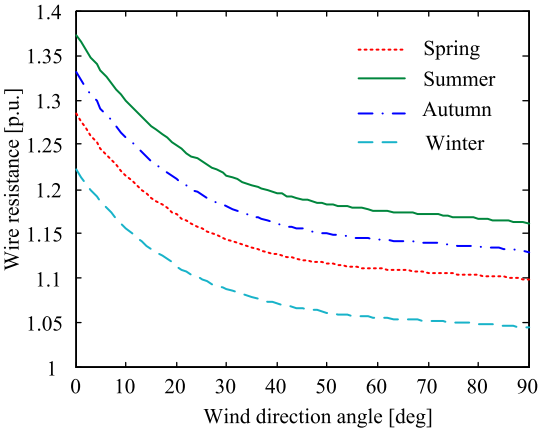

(b) Wind direction angle change

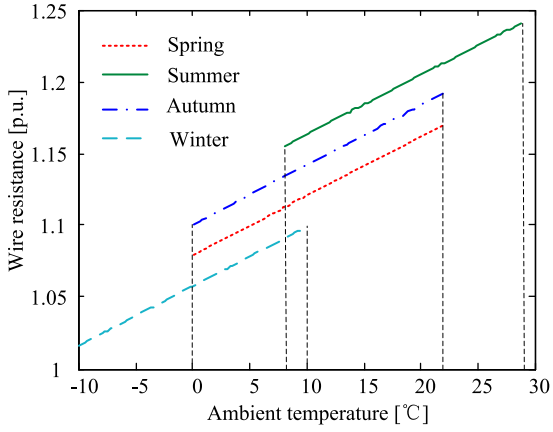

(c) *Ambient temperature change*

FIGURE 7. **Influence of changes in environmental factors on the resistance of the contact wire.**

of environmental parameters on the resistance parameter of the contact wire is studied by controlling the variable. The simulation results are shown in Fig.7. The variation varies within a given range, and the constant parameters adopt the fixed values in Table 1. Figs.7(a), 7(b) and 7(c) show the influence of wind speed, wind direction angle and ambient temperature on the contact wire resistance parameters, respectively. Changes in air density within a small range in the four seasons of the year exert little influence on the wire resistance parameter; hence, such changes are not examined in this study.

Fig. 7 indicates that changes in wind speed, wind direction angle and ambient temperature exert considerable influence on contact wire resistance. As shown in Fig. 7(a), due to the increase in wind speed, the forced convection heat loss is enhanced, and the temperature of the transmission wire is reduced. Thus, the wire resistance decreases with the increase in wind speed. At a low wind speed (less than 5 $m \cdot s^{-1}$), a change in wind speed exerts an obvious influence on the conductor resistance parameters. When the wind speed is high, a change in wind speed exerts no obvious impact on wire resistance mainly due to the influence of forced convection; the temperature of the wire is close to the ambient temperature, and the forced convection heat dissipation is close to saturation. Fig. 7(b) indicates that the wind direction angle affects the convective heat dissipation power of the transmission line. The larger the wind direction angle is, the stronger the convective heat dissipation is. Therefore, the resistance of the conductor decreases with the increase in the wind direction angle. Fig. 7(c) shows that the ambient temperature changes within the variable range in each season. The higher the ambient temperature is, the higher the conductor resistance parameter is. In addition, the relationship between the conductor resistance parameter and ambient temperature is approximately linear. In general, the resistance parameters of the contact wire are relatively high in winter and the lowest in summer due to environmental factors.

Case 2: The environmental parameters under the assumption that the OCS is located in Lhasa are shown in Table 1. The current variation range of the contact wire is 200–800A. Fig. 8 shows the effect of current change on contact wire resistance.

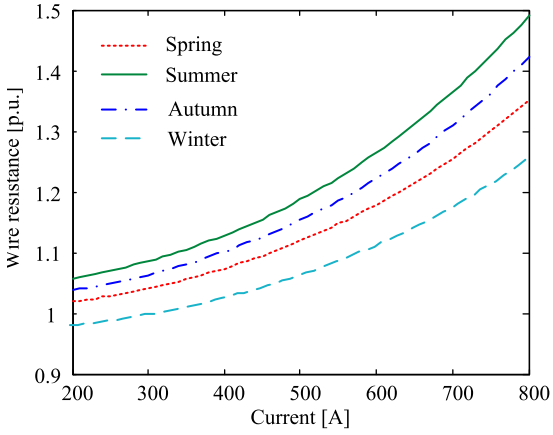

FIGURE 8. **Influence of current change on contact wire resistance.**

It can be seen from Fig. 8 that under certain environmental parameters, the greater the contact wire current, the greater the Joule heat generated, and the higher the wire temperature. Therefore, the resistance of contact wire increases with the increase of current.

Case 3: The environmental parameters use the fixed values of environmental parameters in Lhasa and Nanjing, and the maximum allowable continuous carrying current of the contact wire is calculated under each environmental condition. The simulation results are shown in Fig. 9.

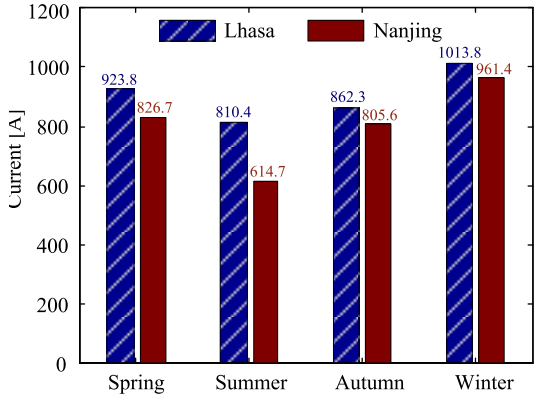

FIGURE 9. Maximum allowable continuous carrying current under different environmental conditions.

Fig. 9 indicates that the difference in geographical and climatic conditions makes the maximum allowable continuous carrying current of contact wire vary considerably. In the same season, the maximum allowable continuous carrying current of the contact wire in the southern locations (e.g. Nanjing) is lower than that of the contact wire in the northern locations (e.g. Lhasa).At the same location, the maximum allowable continuous carrying current of the contact wire in summer is lower than that in winter. Therefore, in the scheduling process, the traction network during peak passenger flow in winter can withstand higher power loads than in summer. When selecting the transmission wires of the traction network, the maximum allowable continuous carrying current of transmission wires should be calculated based on the summer environmental parameters of the area where the traction network is located.

C. ANALYSIS OF THE DYNAMIC CHANGE PROCESS OF RESISTANCE

Case 4: A change in the current of the contact wire (e.g. current change of the train in the process of starting and stopping) and ambient parameters will cause a continuous change in contact wire temperature, which will lead to change in contact wire resistance. Fig. 10 shows the change process of contact wire resistance with current. During the simulation time, the environmental parameters along the traction network are assumed to adopt fixed values in Lhasa (shown in Table 1), and the contact wire is initially in a state of thermal equilibrium. The contact wire current increases from 400A to 600A at 10min and decreases from 600A to 500A at 60min.

Wire resistance is related to wire temperature (Eq. (5)), and the change in wire temperature lags behind the change in current and environmental parameters, which has inertia.

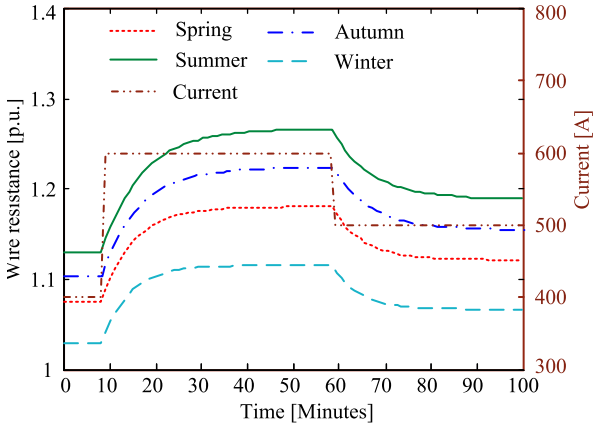

FIGURE 10. Dynamic change process of contact wire resistance with current.

Hence, the change in contact wire resistance in Fig. 10 lags behind the change in current. When the system is in an emergency, the temperature inertia of the conductor can be used to improve the transmission capacity of the wire within a short time in order to gain time for emergency dispatching.

D. POWER FLOW CALCULATION OF THE TRACTION NETWORK IN CONSIDERATION OF THE INFLUENCE OF ELECTRO-THERMAL COUPLING

Analysis of Cases 1 to 4 indicates that the difference in geographical and climatic conditions has a great influence on the resistance and allowable continuous current-carrying capacity of traction network transmission wires. A variation in the transmission wires' resistance inevitably affects the power flow distribution of the traction network. The following example is designed to illustrate the influence of geographical and climatic factors on the power flow of the traction network and verify the effectiveness of the proposed dynamic power flow calculation method that considers the influence of electro-thermal coupling.

Case 5: Suppose that two trains are located 5 and 11km away from the traction substation, and the trains adopt the constant power model. The power of each train is given by P+jQ=8.999+j4.357 MW, and the iterative accuracy is 0.01. In the process of power flow calculation, the environmental parameters use the fixed values of the parameters in Lhasa and Nanjing (Tables 1 and 2). Figs.11(a) and 11(b) show the calculation results of the train terminal voltage at 5 and 11km away from traction substation, respectively, under different geographical and climatic conditions. The voltage shown by the horizontal line in the figures is the result of power flow calculation without considering the effect of electro-thermal coupling in Ref. [28]. In Ref. [28], the impedance of the transmission wires of the traction network was adopted as the impedance under reference environmental conditions, which were constant in the process of power flow calculation; in addition, the influence of geographical and climatic factors on the transmission wires' impedance was not considered.

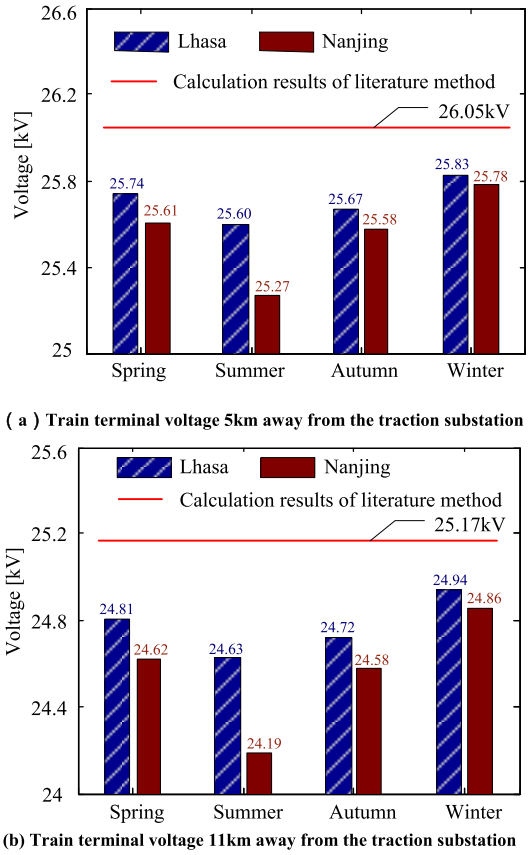

FIGURE 11. Results of power flow calculation of train terminal voltage.

As indicated in Fig. 11, the power flow calculation results without considering the influence of electro-thermal coupling in Ref. [28] are higher than those of the method proposed in this study that considers the influence of electro-thermal coupling. The difference is very large. The main reason is that the temperature of the transmission wire increases due to the effects of current and geographical and climatic conditions, which increase the wire resistance and voltage loss of the traction network. The simulation results are consistent with those of the theoretical analysis, thus proving the rationality of the proposed power flow calculation method.

In Fig. 11, the calculation results of power flow in consideration of the influence of electro-thermal coupling do not vary considerably under different geographical and climatic conditions. The main reason is that the influence of electro-thermal coupling is considered under different geographical and climatic conditions. The conductor temperature is higher than the ambient temperature, and the temperature difference between wires under different conditions is not excessively large; thus, the resistance difference is small. According to the analysis, in the process of power flow calculation of the traction network in consideration of the effect of electro-thermal coupling, the environmental parameters indifferent locations can be averaged, and doing so would exert little influence on the power flow calculation results.

E. PRACTICAL APPLICATION AND BENEFIT ANALYSIS

1) APPLICATION IN THE SELECTION OF TRANSMISSION LINE IN THE TRACTION NETWORK

It can be seen from Figure 9 that the maximum allowable current-carrying capacity of the same transmission line is different under different geographical and climatic conditions. The maximum allowable continuous current-carrying capacity of transmission line in the northern area (such as Lhasa) is higher than that in the southern area (such as Nanjing). The maximum allowable continuous current-carrying capacity of the transmission wire is the main parameter to be considered in the selection process of the transmission line. Therefore, in the selection process of the transmission line in the traction network, the maximum allowable continuous current-carrying capacity of the conductor shall be determined according to the climatic conditions in the area where the transmission wire is located. Sometimes the parameters determined by the climatic and geographical conditions are different from those determined under the limit conditions, thus reducing the installation Cost of transmission wires in the traction network.

2) APPLICATION IN LOAD DISPATCHING OF TRACTION NETWORK

The maximum allowable continuous current-carrying capacity of transmission wire in the traction network in winter is obviously higher than that in summer in the same area. During the spring festival in China, the passenger flow is very large and the load of traction network is increased. The load of the traction network can be increased by taking advantage of the high maximum allowable current-carrying capacity of transmission wire in winter. This operation can save the cost of capacity of transmission wire increase in the traction network and improve the capacity utilization rate of transmission wire in the traction network.

3) APPLICATION IN POWER FLOW CALCULATION IN THE TRACTION POWER SUPPLY SYSTEM

The power flow calculation of the traction power supply system is the basis of judging system stability and optimizing dispatching. In the process of power flow calculation, considering the influence of electric-thermal coupling of the transmission wire will make the power flow calculation results of the traction power supply system more congruent with the reality.

VIII. CONCLUSIONS

In this study, electro-thermal coupling theory was introduced into the traction power supply system, and a method was proposed for the power flow calculation of the traction network that considered the influence of electro-thermal coupling. The specific conclusions are as follows:

(1) Under the influence of electro-thermal coupling, the temperature and the resistance parameters of the transmission wire increase. In the process of wire selection for the

traction network, the maximum allowable continuous carrying capacity of the conductors was the main parameter to be considered. A significant difference was found in the maximum allowable continuous carrying capacities of the wires under different geographical and climatic conditions. This factor needs to be calculated according to the climatic conditions of the different seasons for the traction network.

(2) In the process of the power flow calculation of the traction network, the change in the resistance of the transmission wires should be considered to ensure that the calculation results will be much more accurate and practical.

(3) In this study, the calculation link of the transmission line temperature was introduced into the traditional Newton–Raphson power flow calculation method, and the resistance of the traction network was updated in real time to reflect the change process of the resistance parameters of the transmission wires.

(4) Electro-thermal coupling theory has been widely applied to power systems but not to traction power supply systems. The introduction of electro-thermal coupling theory into the traction power supply system is a new exploration, but it needs to be studied deeply. For example, electro-thermal coupling theory can be applied to the other power flow calculation methods of traction networks, the stress evaluation of the traction network's transmission wires affected by wire heating, and the optimal dispatching of traction power supply systems that consider the effects of electro-thermal coupling. Moreover, the present study is expected provide reference for other scholars in the field.

REFERENCES

[1] H. Banakar, N. Alguacil, and F. D. Galiana, "Electrothermal coordination part I: Theory and implementation schemes," *IEEE Trans. Power Syst.*, vol. 20, no. 2, pp. 798–805, May 2005, doi: 10.1109/TPWRS.2005.846196.

[2] N. Alguacil, M. H. Banakar, and F. D. Galiana, "Electrothermal coordination part II: Case studies," *IEEE Trans. Power Syst.*, vol. 20, no. 4, pp. 1738–1745, Nov. 2005, doi: 10.1109/TPWRS.2005.857836.

[3] I. Theodosoglou, V. Chatziathanasiou, A. Papagiannakis, B. Więcek, and G. De Mey, "Electrothermal analysis and temperature fluctuations' prediction of overhead power lines," *Int. J. Electr. Power Energy Syst.*, vol. 87, pp. 198–210, May 2017, doi: 10.1016/j.ijepes.2016.07.002.

[4] J. Shu, R. Guan, and L. Wu, "Optimal power flow in distribution network considering spatial electro-thermal coupling effect," *IET Gener., Transmiss. Distrib.*, vol. 11, no. 5, pp. 1162–1169, Mar. 2017, doi: 10.1049/iet-gtd.2016.0909.

[5] S. Frank, J. Sexauer, and S. Mohagheghi, "Temperature-dependent power flow," *IEEE Trans. Power Syst.*, vol. 28, no. 4, pp. 4007–4018, Nov. 2013, doi: 10.1109/TPWRS.2013.2266409.

[6] M.-X. Wang and X.-S. Han, "Study on electro-thermal coupling optimal power flow model and its simplification," in *Proc. IEEE PES Gen. Meeting*, Providence, RI, USA, Jul. 2010, pp. 25–29.

[7] R. Olsen, J. Holboell, and U. S. Gudmundsdottir, "Electrothermal coordination in cable based transmission grids," *IEEE Trans. Power Syst.*, vol. 28, no. 4, pp. 4867–4874, Nov. 2013, doi: 10.1109/TPWRS.2013.2278040.

[8] X. M. Dong, C. Q. Kang, Y. Y. Ding, and C. F. Wang, "Estimating the wind power integration threshold considering electro-thermal coupling of overhead transmission lines," *IEEE Trans. Power Syst.*, vol. 34, no. 5, pp. 3349–3357, Sep. 2019, doi: 10.1109/TPWRS.2019.2906291.

[9] A. Ahmed, F. S. McFadden, and R. Rayudu, "Impacts of distributed PV in a smart grid using temperature-dependent power flow," in *Proc. IEEE Innov. Smart Grid Technol. Asia (ISGT-Asia)*, Auckland, New Zealand, Dec. 2017, pp. 4–7.

[10] D. M. Greenwood and P. C. Taylor, "Investigating the impact of real-time thermal ratings on power network reliability," *IEEE Trans. Power Syst.*, vol. 29, no. 5, pp. 2460–2468, Sep. 2014, doi: 10.1109/TPWRS.2014.2305872.

[11] J.-A. Jiang, Y.-T. Liang, C.-P. Chen, X.-Y. Zheng, C.-L. Chuang, and C.-H. Wang, "On dispatching line ampacities of power grids using weather-based conductor temperature forecasts," *IEEE Trans. Smart Grid*, vol. 9, no. 1, pp. 406–415, Jan. 2018, doi: 10.1109/TSG.2016.2553964.

[12] A. Safdarian, M. Z. Degefa, M. Fotuhi-Firuzabad, and M. Lehtonen, "Benefits of real-time monitoring to distribution systems: Dynamic thermal rating," *IEEE Trans. Smart Grid*, vol. 6, no. 4, pp. 2023–2031, Jul. 2015, doi: 10.1109/TSG.2015.2393366.

[13] M. Wang, M. Yang, J. Wang, M. Wang, and X. Han, "Contingency analysis considering the transient thermal behavior of overhead transmission lines," *IEEE Trans. Power Syst.*, vol. 33, no. 5, pp. 4982–4993, Sep. 2018, doi: 10.1109/TPWRS.2018.2812826.

[14] X. L. Yu, H. X. Zhang, and M. X. Wang, "An algorithm for power system state estimation considering line temperature," *Zhongguo Dianji Gongcheng Xuebao*, vol. 38, no. 9, pp. 2561–2570, May 2018, doi: 10.13334/j.0258-8013.pcsee.171161.

[15] H. Hu, Z. He, X. Li, K. Wang, and S. Gao, "Power-quality impact assessment for high-speed railway associated with high-speed trains using train timetable—Part I: Methodology and modeling," *IEEE Trans. Power Del.*, vol. 31, no. 2, pp. 693–703, Apr. 2016, doi: 10.1109/TPWRD.2015.2472994.

[16] H. Lee, C. Lee, G. Jang, and S. Kwon, "Harmonic analysis of the Korean high-speed railway using the eight-port representation model," *IEEE Trans. Power Del.*, vol. 21, no. 2, pp. 979–986, Apr. 2006, doi: 10.1109/TPWRD.2006.870985.

[17] L. Guo, Q. Li, and Y. Xu, "Study on harmonic resonance of traction line in electrified high-speed traction system," in *Proc. Int. Conf. Sustain. Power Gener. Supply*, Nanjing, China, Apr. 2009, pp. 6–7.

[18] S.-H. Lee, J.-O. Kim, and H.-S. Jung, "Analysis of catenary voltage of an AT-fed AC HSR system," *IEEE Trans. Veh. Technol.*, vol. 53, no. 6, pp. 1856–1862, Nov. 2004, doi: 10.1109/TVT.2004.836932.

[19] T. K. Ho, Y. L. Chi, J. Wang, K. K. Leung, L. K. Siu, and C. T. Tse, "Probabilistic load flow in AC electrified railways," *IEE Proc. Electr. Power. Appl.*, vol. 152, no. 4, pp. 1003–1013, Jul. 2005, doi: 10.1049/ip-epa:20045091.

[20] L. Battistelli, M. Pagano, and D. Proto, "2 × 25-kV 50 hz high-speed traction power system: Short-circuit modeling," *IEEE Trans. Power Del.*, vol. 26, no. 3, pp. 1459–1466, Jul. 2011, doi: 10.1109/TPWRD.2010.2100832.

[21] M. Wu, "Uniform chain circuit model for traction networks of electric railways," *Proc. CSEE*, vol. 30, no. 28, pp. 52–58, Oct. 2010.

[22] J. W. He, Q. Z. Li, W. Liu, and X. H. Zhou, "General mathematical model for simulation of AC traction power supply system and its application," *Dianwang Jishu*, vol. 34, no. 7, pp. 25–29, Jul. 2010.

[23] H. Hu, Y. Shao, L. Tang, J. Ma, Z. He, and S. Gao, "Overview of harmonic and resonance in railway electrification systems," *IEEE Trans. Ind. Appl.*, vol. 54, no. 5, pp. 5227–5245, Sep. 2018, doi: 10.1109/TIA.2018.2813967.

[24] J. Q. Zhang and M. L. Wu, "Power flow algorithm for electric railway traction network based on multiple load port Thévenin equivalence," *Diangong Jishu Xuebao*, vol. 33, no. 11, pp. 2479–2485, Jun. 2018, doi: 10.19595/j.cnki.1000-6753.tces.170501.

[25] Q. Z. Li, D. Yi, and J. M. He, "Power supply capacity of traction cable for Ac electrified railway," *Xinan Jiaotong Daxue Xuebao*, vol. 48, no. 1, pp. 81–87, Feb. 2013, doi: 10.3969/j.issn.0258-2724.2013.01.013.

[26] *IEEE Standard for Calculating the Current-Temperature Relationship of Bare Overhead Conductors*, IEEE Standard 738, 2012.

[27] C. R. Black and W. A. Chisholm, "Key considerations for the selection of dynamic thermal line rating systems," *IEEE Trans. Power Del.*, vol. 30, no. 5, pp. 2154–2162, Oct. 2015, doi: 10.1109/TPWRD.2014.2376275.

[28] F. Wang and X. R. Wang, "A power flow analysis method of traction power supply system based on constant—Power Load," *Proc. CSU-EPSA*, vol. 27, no. 3, pp. 59–64, Mar. 2015, doi: 10.3969/j.issn.1003-8930.2015.03.11.

LIJUN SUN was born in ChangChun, JiLin, China, in 1984. He received the bachelor's and M.S. degrees in automation and electrical engineering from Lanzhou Jiaotong University, China, in 2007 and 2013, respectively. He is currently a Lecturer with the Department of Key Laboratory of Opto-Technology and Intelligent Control Ministry of Education, Lanzhou Jiaotong University, China. His main research interests are in power flow analysis and energy saving optimization of traction power supply systems.

RUOPENG ZHANG was born in Jinchang, Gansu, China, in 1996. He received the bachelor's in Bowen College from Lanzhou Jiaotong University, China, in 2018. He is currently a graduate student with the Department of School of Automation & Electrical Engineering, Lanzhou Jiaotong University, China. His main research interests are in Power flow calculation of traction power supply systems.

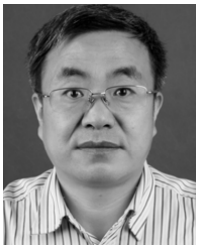

MINGXING TIAN was born in Minqin, Gansu, China, in 1968. He received the bachelor's degree in electric traction and drive control from North Jiaotong University, China, in 1990. He received the M.S. degree in power transmission and automation from Southwest Jiaotong University, China, in 1997. He received the doctor's degree in electrical engineering from Xi'an Jiaotong University, China, in 1997. He is currently a professor with the department of School of Automation & Electrical Engineering, Lanzhou Jiaotong University, China. His main research interests are in power quality analysis and control of power system, motor design, etc.

HUIYING ZHANG was born in Shangqiu, Henan, China, in 1980. She received the bachelor's and M.S. degrees in School of Automation & Electrical Engineering, from Henan Polytechnic University, China, in 2003 and 2008, respectively. She is currently a doctor with the Department of School of Automation & Electrical Engineering, Lanzhou Jiaotong University, China. Her main research interests are in parameter calculation of transmission line in traction networks.

WENJUN TIAN was born in Minqin, Gansu, China, in 1985. She received the bachelor's and M.S. degrees in automation and electrical engineering from Lanzhou Jiaotong University, China, in 2008 and 2011, respectively. She is currently a lecturer with the department of School of Automation & Electrical Engineering, Lanzhou Jiaotong University, China. Her main research interests are in analysis and treatment of power quality in traction power supply systems.

JINYANG XU was born in Heping, Guangdong, China, in 1993. He received the bachelor's degree in automation and electrical engineering from SouthWest Jiaotong University, China, in 2001. He received the M.S. degree in automation and electrical engineering from Lanzhou Jiaotong University, China, in 2007. He is currently a lecturer with the department of School of Automation & Electrical Engineering, Lanzhou Jiaotong University, China. His main research interest is in power theory analysis.